Validation of a PCM Simulation Tool in IDA ICE Dynamic Building Simulation Software Using Experimental Data from Solar Test Boxes

Cristina Cornaro – Tor Vergata University – cornaro@uniroma2.it
Marco Pierro – Tor Vergata University – marco.pierro@uniroma2.it
Daniele Roncarati – Tor Vergata University – daniele.roncarati3@gmail.com
Valerio Puggioni – EnUp – puggioni@enup.it

Abstract

This work aims to provide a method to validate a PCM tool implemented in a whole building dynamic simulation software (IDA ICE) using outdoor measurements coming from Solar Test Boxes (STB).

The STB method was originally conceived by ESTER lab at the University of Rome Tor Vergata, to evaluate thermal characteristics of transparent and semi transparent materials in outdoor conditions. In the approach presented here, two boxes (reference and test) were equipped with a standard double glass pane. A PCM pane, provided by RUBITHERM®, was put on the floor of the test box. Two monitoring campaigns were carried out and the thermal behaviour of the box with PCM was analyzed and compared with the thermal behaviour of the reference box. Temperature trends measured inside the "PCM box" were used to validate the PCM behaviour provided by the IDA ICE tool, comparing measured and simulated data.

1. Introduction

Since the 1930s Phase Change Materials (PCM) have been investigated thanks to the pioneering work of Telkes (1975). Many studies have been conducted on these materials since then but unfortunately their application did not take off due to technological constraint and costs. However, as recent reviews show (Khadiran et al., 2016; Souayfane et al., 2016), interest for PCM has increased again in the last years.

Many studies can be found in the literature regarding experimental and theoretical analyses of PCM behavior. It is possible to group these works into laboratory experimental activity, outdoor experimental activity, numerical and theoretical investigation and studies involving experiments and theory.

Various works can be found on laboratory tests. Most of the examined works regard the evaluation of the thermal characteristics of gypsum boards containing microencapsulated PCM tested in simulation chambers and/or tests boxes (Lee at al., 2007; Zhang et al., 2012, 2013; Li et al., 2013; Marchi et al., 2013). Barreneche et al. (2013) incorporated PCMs with Portland cement and gypsum and investigated the best PCM quantity to be incorporated for each tested material.

The paper by Tardieu et al. (2011) on outdoor experimental activity that used two cabins built in Auckland, New Zealand, is worth mentioning. One was used as reference and one with PCM and numerical simulation using Energy Plus to evaluate the thermal behavior of the two cabins. Both simulation and experimental data collected showed that PCM in wallboards improved the thermal inertia of buildings. From simulations they also concluded that the additional thermal mass of PCM can reduce the daily indoor temperature fluctuation by up to 4 °C in summer days. Also Entrop et al. (2011) made experiments using small outdoor boxes in Denmark, equipped with different materials among which, PCM. Their results evidenced that PCM is an excellent way to store energy and small boxes are effective in studying this aspect. Also Su et al. (2012) used a box to evaluate the PCM thermal behavior in China, while Sage-Lauck and Sailor (2014) built a passive house duplex in Portland, Oregon. They found that the addition of PCM could reduce by about 60 % the over-heating number hours.

Goia et al. (2014) tested a glazing system filled with PCM in outdoor conditions during a long term monitoring campaign. They concluded that the PCM glazing is capable of smoothing and shifting solar gains, and that this result could positively contribute to the energy balance of highly glazed buildings. Numerical simulation is also used to evaluate PCM performance at different locations and climates using various simulation tools such as ESP-r (Fernandez and Costa, 2009), self-made programs (Zwanzig et al., 2013), COMSOL environment (Zhou et al., 2014), and Energy Plus (Guarino et al., 2015). All these works should be supported by experimental data as by Guarino et al. (2015).

The aim of this work is to provide valuable experimental data that could be used to validate the behavior of a custom PCM simulation tool integrated in the whole building simulation software IDA ICE by EQUA simulation. In the following sections the experimental facility used for the study is presented together with the custom PCM software module implemented in the IDA ICE environment. We introduce the results of the monitoring campaigns, and discuss a comparison between simulated and measured data to validate the tool. Once validated, the software module could be used to evaluate energy performance of PCM in buildings.

2. Simulation and Experiment

2.1 Method

Solar Test Boxes (STBs) were built with the objective of carrying out a comparative analysis of thermal and lighting performance of transparent material with respect to a double glass reference pane, and to evaluate solar heat gain and U-value of the innovative semi-transparent materials. In the present study they were used to test the thermal performance of a SP21E PCM pane provided by RUBITHERM®, the characteristics of which are listed in Table 1. The STBs were provided with two identical standard double glass panes. In the experiments one of the boxes (PCM) contained the PCM panel while the other (Ref) was used as a reference.

Table 1 – SP21E PCM pane characteristics

Data	Value
Melting area	22–23 °C
Congealing area	21–19 °C
Heat Storage Capacity Combination of sensible and latent heat in a temperature range of 13 °C to 28 °C.	160 kJ/kg
Specific Heat Capacity	2 kJ/(kg K)
Density solid (15 °C)	1.5 kg/l
Density liquid (35 °C)	1.4 kg/l
Volume expansion	3–4 %
Thermal conductivity	0.6 W/(m K)
Max Operation temperature	45 °C

The STBs thermal behaviour was simulated in the IDA ICE dynamic simulation environment. In particular the PCM box model was provided with the custom PCM software module to simulate the PCM pane. The temperature data, gathered during two short-term outdoor monitoring campaigns, carried out in different periods of the year, were used to validate the results.

2.2 Solar Test Boxes Description

The boxes were designed with a linear scale factor of 1:5 and a surface scale factor of 1:25 with respect to a real room. They have the dimensions of 1.00 m × 0.60 m × 0.55 m and consist of 5 opaque walls and one glazed wall. The exterior was manufactured with plywood panels of 8 mm thickness painted entirely white, to make them highly reflective. The entire not glazed inner surface of the boxes, also comprising the portion of the area behind the frame of the window, was heavily insulated with a lightweight rigid insulating material of 80 mm thickness, Stiferite GT, specific for thermal insulation in buildings. On the south facing wall a glazed area of 42 cm × 37 cm can be allocated, the remaining of this surface being occupied by a wood frame 90 mm thick, to shield the thickness of the inside insulating panes.

Table 2 – Thermal properties of STB materials

	Thickness (mm)	Density (kg/m³)	Specific heat (J/(kg K))	Thermal conductivity (W/(m K))	Thermal resistance (m²K/W)	SHGC
Plywood	8	545	1215	0.120	-	-
Insulation	80	36	1453	0.024 (at 10 °C)	3.33	-
Double glazed pane	20	2400	800	1.4	0.34	0.82

Each box is equipped to measure inside air temperature, illuminance, and surface temperature of the inner and outer side of the glazed pane.
Temperature sensors are TT500 thermistors by Tecno.el srl with a wide temperature range (-30 to 120 °C), a resolution of 0.1 °C and an accuracy of ±0.2 °C. Illuminance is measured using a luxmeter by Delta Ohm srl with a measurement range of 200,000 lx, a sensitivity of 1.5 mV/klx and a less than 4 % calibration accuracy less than 4 W/%. Also outside temperature and relative humidity, solar irradiance on the vertical plane, and wind speed and direction are measured using a portable weather station. Temperature and relative humidity are measured by a Rotronic Hygroclip2 sensor with a ±0.1 °C accuracy for the temperature, and a ±0.8 % accuracy for relative humidity. The solar irradiance sensor is a silicon cell pyranometer provided by Apogee Instruments with an accuracy of ±5 % while wind speed and direction are measured using a 7911 anemometer model provided by Davis Instruments with an accuracy of ±1 m/s for speed and of ±7 ° for direction. Data are acquired at a minute time rate.
The weather and solar station of ESTER lab (Lat. 41.9, Long. 12.6) provides direct and diffuse solar irradiance measurements useful for climate file construction in dynamic simulation software. Table 2 lists the material properties used in STBs.

2.3 STB Calibration

STBs original calibration is reported in Cornaro et al., 2015. For the purpose of this study it was necessary to reduce the glazed surface to control solar irradiance entering the boxes. In this way PCM was not exposed to too high temperatures that could damage it. For this reason, the original glazed area was reduced using a wider wood frame. A new calibration was then necessary to take this modification into account (Fig. 1).

Fig. 1 – STBs with different window frames during the calibration test

A short – term monitoring campaign was carried out at ESTER lab from November 12 to 17, 2015, to collect calibration data.
Fig. 2 shows the trends of the external and inside air temperatures, monitored in the two STBs equipped with the reference glazed pane and the two different frames. The inside temperature of both boxes increased to 50 °C and more, due to the high insulation properties of the materials and the solar heat gain of the glazing. In particular, the inside temperature of the old framed STB (Tair_OF) reached almost 80 °C, or more, while the new framed STB (Tair_NF) did not exceed 50 °C. This difference is explained by the reduction of the glazed surface due to the new frame.
First of all the air temperature trend inside the old framed box was compared to the simulation data provided by the STB model to verify the old calibration accuracy. Root mean square error (RMSE) and normalized RMSE, NMRSE, were used to evaluate the accuracy. The two indexes are defined as:

$$\mathrm{RMSE} = \sqrt{\frac{\sum_{i=1}^{n}(x_i^m - x_i^s)^2}{n}} \quad (1)$$

$$\mathrm{NRMSE} = \frac{RMSE}{x_{max}^m - x_{min}^m} \quad (2)$$

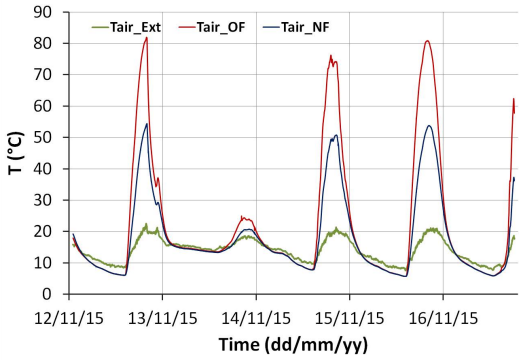

Fig. 2 – Temperature trends recorded during the calibration of the new frame (NF); OF = original frame; Ext = outside air

A RMSE of 2.72 °C was obtained over the whole test period with a 4 % NRMSE indicating good agreement with the original calibration.

To calibrate the new framed box the inside air temperature obtained by the STB simulation model was compared with the experimental data; the U-value of the frame and the ratio of opaque over glazed area (frame fraction) were changed in the model till the RMSE reached a minimum. Fig. 3 shows the inside air temperature trends of the new framed STB after calibration. A RMSE of 2.56 °C was obtained with a 5.4 % NRMSE, considering a U = 2 W/(m²K) and a frame fraction, F = 0.55.

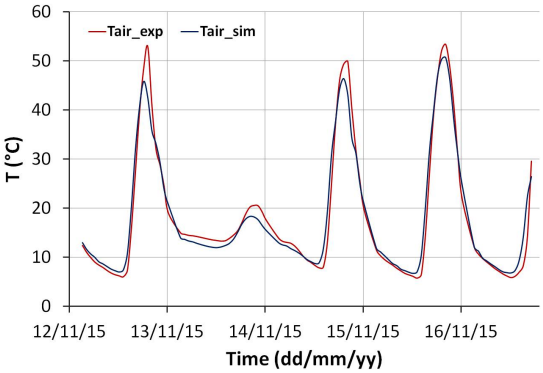

Fig. 3 – Comparison between measured and simulated temperature trends inside the new framed box after calibration

2.4 Measurement Campaigns

Two masurement campaigns were carried out, each of them including three full days of data acquisition.

2.4.1 First campaign

The first campaign was conducted from September 26 to 29, 2016. Two boxes were exposed outdoor, one with a PCM pane layered on the box floor (PCM box) and the other one without PCM (Ref box). Air temperature inside both boxes was measured together with outdoor air temperature, relative humidity, wind speed and direction, and global irradiance on a vertical plane. Climatic conditions during the test are presented in Fig. 4 with air temperature (Tair_ext) and solar irradiance measured on a vertical plane (GR_V). Good weather conditions characterized the period with high temperatures (maximum peak at 29 °C) and a significant thermal range between day and night (12–13 °C). Solar irradiance reached peaks of approx. 800 W/m². Fig. 5 shows the air temperature trends inside the reference box (Tair_ref) and the PCM box (Tair_PCM) during the test. A significant decrease in maximum temperature is observed in the PCM box when compared to Ref box due to the PCM melting in the 22–23 °C temperature range. An average decrease of the temperature peaks of approx. 10 °C is observed during the day while at night the opposite behavior occurs. Indeed, the air temperature inside the PCM box is higher than in the Ref box due to the PCM solidification and the thermal mass.

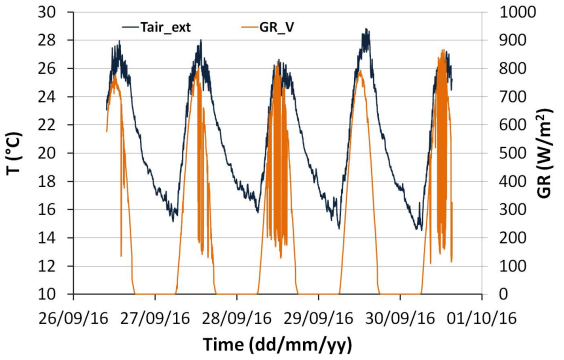

Fig. 4 – Outdoor air temperature and global irradiance on a vertical plane experienced during the first measurement campaign

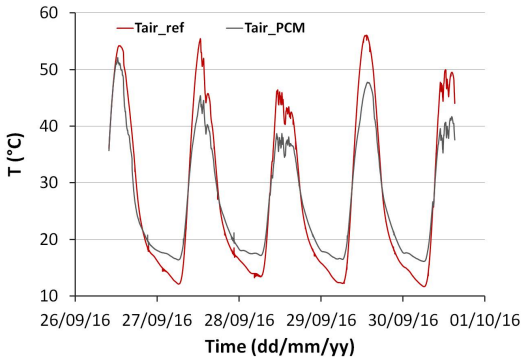

Fig. 5 – Air temperature inside the Ref box and the PCM box during the first test

No evident shift of the temperature trend due to PCM heat capacity is observed, that is because the amount of material in the box is not enough to produce this effect.

2.4.2 Second campaign

A second measurement campaign was carried out later, in winter, between December 5 and 9, 2016. We experienced nice weather during the last two days of test while the first day was overcast but not rainy, as evidenced by Fig. 6. The outdoor air temperature, in this case, was lower than in the first campaign with a maximum of approx. 21 °C, and a minimum of approx. 2 °C with a thermal range of 15 °C in the clear days. Solar irradiance reached values as high as 930 W/m². This is because in this period the sun elevation is low so a vertical surface receives higher irradiance than a horizontal one.
Fig. 7 shows the temperature trends inside Ref and PCM boxes.

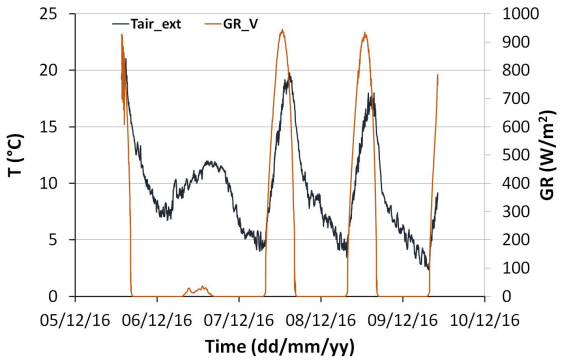

Fig. 6 – Outdoor air temperature and global irradiance on a vertical plane experienced during the second measurement campaign

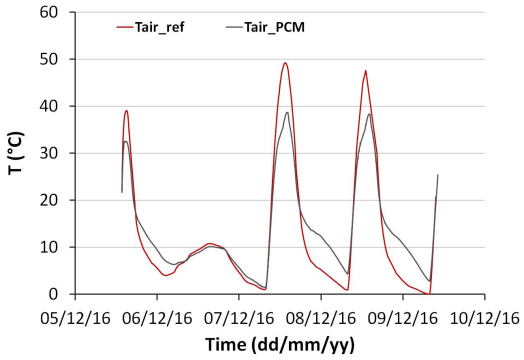

Fig. 7 – Air temperature inside the Ref box and the PCM box during the second test

Also in this case a temperature peak damping of approx. 10 °C caused by the PCM is observed during the clear days, while for the overcast day no effect of the material is observed due to the low temperatures experienced inside the box (well below melting point). PCM solidification occurs earlier in the day (around 7 pm) than in the first campaign (around midnight). Apart from this shift, we also observed a change in the curvature of the decreasing temperature trend with respect to the first campaign. This is probably due to the behavior of the solid phase at temperatures well below the solidification.

2.5 Simulation

2.5.1 STB model

STBs were simulated in the IDA ICE environment. The geographic location corresponded to ESTER lab coordinates, and customized climate files were built for all the simulations using weather data coming from the weather and solar station of the same lab. The boxes were oriented with the glazing area toward south. The thermal properties presented in Table 2 were inserted in the model. For what concerns the STB provided with the PCM, the custom software module was connected to the STB floor working in advanced level mode.

2.5.2 Custom PCM software module description

"PCM wall" is a module for IDA ICE, written in NMF language (Neutral Model Format), that allows calculating heat absorbed and/or released by phase change materials. It uses an enthalpy formulation to describe the relation between enthalpy and temperature for a PCM material with different paths during melting and solidifying phases. The partial enthalpies and the temperature coordinates are input parameter vectors describing this relation. Partial enthalpies are expressed in J/kg. Heat capacity (J/(kg K)) is calculated by dividing the partial enthalpies difference at different temperatures by the correspondent temperature interval.
The computed help variable "Mode" is used to keep track of the current state (phase) of the PCM material.

There are five different PCM conditions that can be monitored with the variable "Mode", for which heat capacity, thermal resistance, and temperature as a function of enthalpy are computed:

- Mode -2: solid phase
- Mode 2: liquid phase
- Mode -1: solidifying phase
- Mode 0: reversing during melting/solidifying phase
- Mode 1: melting phase

Fig. 8 shows the enthalpy versus temperature curves, as specified by RUBITHERM® for the SP21 PCM pane, for heating and cooling. These data were input to the PCM software module.

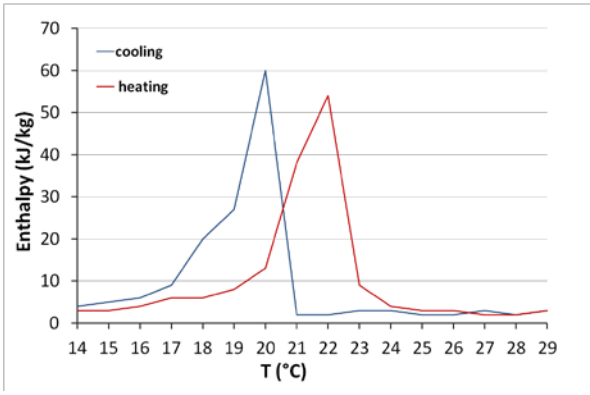

Fig. 8 – Enthalpy – Temperature curves for heating and cooling for the tested SP21 PCM pane

3. Discussion and Results

Experimental data gathered during the two experimental campaigns were used to validate the custom PCM software module with two datasets in which the PCM behaved in different ways due to different climatic conditions. During the first campaign, in the month of September, the weather conditions were such that the PCM material could work fully in its phase change temperature range, while in the month of December, even if solar irradiance was high, external air temperature limited the PCM phase status mainly to solid for most of the period. Fig. 9 A and B show the comparison between the experimental and simulated temperature trends inside the PCM box for the campaign of September and December, respectively. A very good agreement can be observed for both periods indicating the correct simulation of the boxes and the PCM. In Fig. 9B a major difference between the experimental and simulated temperature is observed during the night, when the air temperature inside the PCM box fell to 18 °C. In this period the PCM material is in the solid phase and it continues to cool down. The model does not seem to follow the experimental trend as well as during the first campaign, this is probably due to the fact that the PCM specifications are not available in the model for such low temperatures.

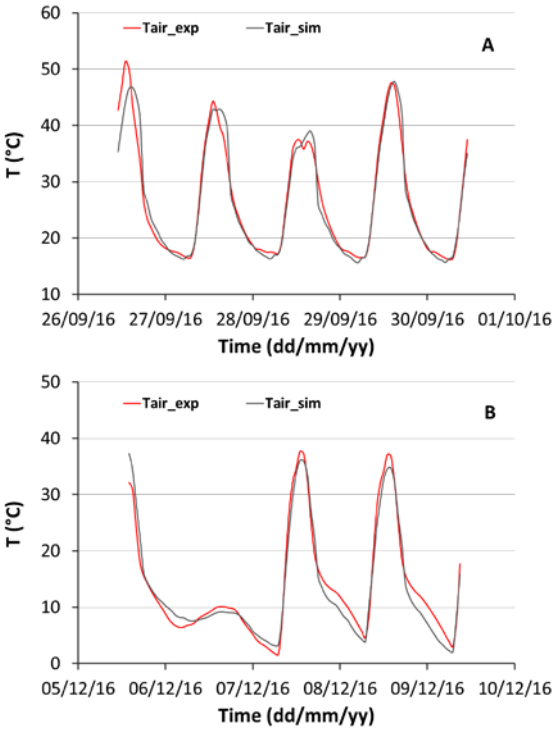

Fig. 9 – Measured and simulated air temperature, inside the PCM box for the first (A) and second (B) monitoring campaign

When overcast, day temperatures were too low so the PCM always remained in the solid phase. To quantify the accuracy of the simulation, we evaluated the RMSE and NMRSE for all cases, and listed them in Table 3. In the calculations the first and last hours of operation were discarded to evaluate the indexes on three full days for each campaign. Also the indexes referred to Ref box were evaluated to verify the correct simulation of the box itself. It can noticed how NRMSE stays below 6 % in all cases, confirming the optimum agreement.

Table 3 – RMSE and NMRSE between measured and simulated temperature trends for the two campaigns

Campaign	Ref box		PCM box	
	RMSE (°C)	NMRSE (%)	RMSE (°C)	NMRSE (%)
26-29/09/16	1.78	4.1	1.57	5.0
05-12/12/16	2.50	5.2	1.83	5.1

Fig. 10 A and B show the heat fluxes (HF) of PCM and of the incoming solar radiation together with the temperature experienced by PCM simulated for the two monitoring campaigns.

The pane removes approx. 15 W peak during the day compared to an incoming solar flux with peaks of around 40 W (around 40 % heat reduction) lowering the box air temperature peaks of approx. 10 °C.

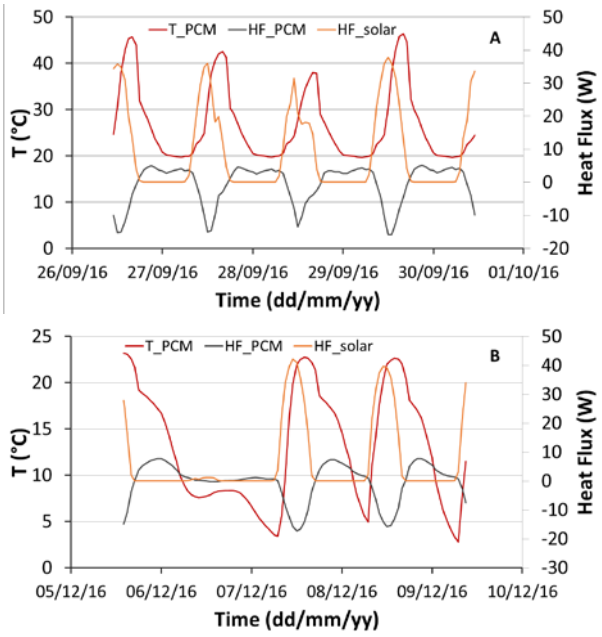

Fig. 10 – Heat flux (HF) of PCM and of incoming solar radiation and temperature trend of the PCM. A: first test; B: second test

During the night it releases heat (4–5 W) due to solidification. While during the first campaign it stays in the liquid phase all day, and in the solid phase during night, in the second campaign it is mainly in the solid phase due to low outside temperatures, melting occurring only between 11:00 am and 6:00 pm.

4. Conclusion

We have introduced a method to validate custom-made software module to simulate PCM materials. The software module was built in the IDA ICE environment and experimental data for validation were collected in two outdoor monitoring campaigns using solar text boxes. A different behaviour of the PCM could be observed due to different climate conditions during the two campaigns. We detected a very good agreement between measured and simulated temperature trends inside the boxes, which proves the good implementation of the customized software module. Small discrepancies were only identified during nighttime for the December campaign, probably due to lack of information on PCM behaviour at such low temperatures in the solid phase. However, this does not invalidate the results obtained. We also carried out the analysis of heat fluxes using the validated model. Future work will consist in the energy saving capability evaluation of PCM materials implemented in office buildings.

References

Barreneche, C., M.E. Navarro, A. Ines Fernandez, L.F. Cabeza. 2013. "Improvement of the thermal inertia of building materials incorporation PCM. Evaluation in the macroscale". *Applied Energy* 109:428–432.doi: 10.1016/j.apenergy.2012.12.055.

Cornaro, C., F. Bucci, M. Pierro, M.E. Bonadonna, G. Siniscalco. 2015. "A new method for the thermal characterization of transparent and semi-transparent materials using outdoor measurements and dynamic simulation". *Energy and Buildings* 104: 57–64. doi: 10.1016/j.enbuild.2015.06.081.

Entrop, A.G., H.J.H. Brouwers, A.H.M.E. Reinders. 2011. "Experimental research on the use of micro-encapsulated Phase Change Materials to store solar energy in concrete floors and to save energy in Dutch houses". *Solar Energy* 85: 1007–1020. doi: 10.1016/j.solener.2011.02.017.

Fernandez, N.T.A., V.A.F. Costa. 2009. "Use of phase-change materials as passive elements for climatization purposes in summer: the

Portuguese case". *International Journal of Green Energy* 6(3):302–311. doi: 10.1080/15435070902886585.

Goia, F., M. Perino, V. Serra. 2014. "Experimental analysis of the energy performance of a full-scale PCM glazing prototype". *Solar Energy* 100: 217–233. doi: 10.1016/j.solener.2013.12.002.

Guarino, F., V. Dermardiros, Y. Chen, J. Rao, A. Athienitis, M. Cellura, M. Mistretta. 2015. "PCM thermal energy storage in buildings: experimental study and applications". *Energy Procedia* 70: 219 – 228. doi: 10.1016/j.egypro.2015.02.118.

Khadiran, T., M.Z. Hussein, Z. Zainal, R. Rusli. 2016. "Advanced energy storage materials for building applications and their thermal performance characterization: a review". *Renewable and Sustainable Energy Reviews* 57: 916–928. doi: 10.1016/j.rser.2015.12.081.

Lee, S.H., S.J. Yoon, Y.G. Kim, Y.C. Choi, J.H. Kim, J.G. Lee. 2007. "Development of building materials by using micro-encapsulated phase change material". *Korean Journal of Chemical Engineering* 24(2):332–5. doi: 10.1007/s11814-007-5054-8.

Li, M, Z. Wu, J. Tan. 2013. "Heat storage properties of the cement mortar incorporated with composite phase change material". *Applied Energy* 103:393–399. doi: 10.1016/j.apenergy.2012.09.057.

Marchi, S., S. Pagliolico, G. Sassi. 2013. "Characterization of panels containing microencapsulated phase change materials". *Energy Conversion and Management* 74:261–268. doi: 10.1016/j.enconman.2013.05.027.

Sage-Lauck, J.S., D.J. Sailor. 2014. "Evaluation of phase change materials for improving thermal comfort in a super-insulated residential building". *Energy and Buildings* 79:32–40. doi: 10.1016/j.enbuild.2014.04.028.

Souayfane, F., F. Fardoun, P.H. Biwole. 2016. "Phase change materials (PCM) for cooling applications in buildings: A review". *Energy and Buildings* 129: 396–431. doi: 10.1016/j.enbuild.2016.04.006.

Su, J.F., X.Y. Wang, S.B. Wang, Y.H. Zhao, Z. Huang. 2012. "Fabrication and properties of microencapsulated-paraffin/gypsum-matrix building materials for thermal energy storage". *Energy Conversion and Management* 55:101–107. doi: 10.1016/j.enconman.2011.10.015.

Tardieu, A., S. Behzadi, J.J.J. Chenand, M.M. Farid. 2011. "Computer simulation and experimental measurements for an experimental PCM-impregnated office building". In: *Proceedings of Building Simulation 2011*. Sydney, Australia: IBPSA.

Telkes, M. 1975. "Thermal storage for solar heating and cooling". In: *Proceeding of the workshop on Solar Energy Storage Subsystems for the Heating and cooling of Buildings.* Charlottesville, U.S.A.

Zhang, G.H., S.A.F. Bon, C.Y. Zhao. 2012. "Synthesis, characterization and thermal properties of novel nano encapsulated phase change materials for thermal energy storage". *Solar Energy* 86:1149–1154. doi: 10.1016/j.solener.2012.01.003.

Zhang, Z., G. Shi, S. Wang, X. Fang, X. Liu. 2013. "Thermal energy storage cement mortar containing n-octadecane/expanded graphite composite phase change material". *Renewable Energy* 50:670–675. doi: 10.1016/j.renene.2012.08.024.

Zhou, D., G.S.F. Shire, Y. Tian. 2014. "Parametric analysis of influencing factors in phase change material wallboard (PCMW)". *Applied Energy* 19:33–42. doi: 10.1016/j.apenergy.2013.12.059.

Zwanzig, S.D., Y. Lian, E.G. Brehob. 2013. "Numerical simulation of phase change material composite wallboard in a multi-layered building envelope". *Energy Conversion and Management* 69:27–40. doi: 10.1016/j.enconman.2013.02.003.